Proceedings of the Twenty-eighth (2018) International Ocean and Polar Engineering Conference
Sapporo, Japan, June 10-15, 2018

ISBN 978-1-880653-87-6; ISSN 1098-6189

www.isope.org

Numerical Study of a Fixed FPSO-Shaped Body under Focused Waves with Different Headings

*Yuan Zhuang, Qi Li, Decheng Wan**

State Key Laboratory of Ocean Engineering, School of Naval Architecture, Ocean and Civil Engineering, Shanghai Jiao Tong University, Collaborative Innovation Center for Advanced Ship and Deep-Sea Exploration, Shanghai, China
*Corresponding author

ABSTRACT

This paper applies our in-house solver, naoe-FOAM-SJTU to simulate a fixed FPSO-shaped body in focused waves. This benchmark test follows the settings of experiments conducted in the Ocean Basin at Plymouth University's COAST Laboratory. The different headings are considered to figure out how the focused waves influence the fixed model. The values of wave height in different position of the empty wave tank are obtained through computations to compare with the experimental results. The scattered wave height and impact pressure on the hull are provided. The results of the wave and the corresponding pressure on the hull are in CCP-WSI Blind Test Workshop to ensure the accuracy of the method. It is found that the incident wave angle affects the maximum crest height and wave loading.

KEY WORDS: gap flow; side-by-side; CFD method; naoe-FOAM-SJTU solver

INTRODUCTION

As for offshore structures, it's essential to study those structures operating under the hostile environment. On the one hand, the designation and operation need to avoid structure damage and loss on work stoppage, thus the severe sea states must be considered. For example, the FPSO in deep sea may encounter with magnificent wave height, which may cause damage to ship bow. On the other hand, the wave-wave interaction may transfer high-frequency energy to the structure. Those wave-induced high-frequencies may cause nonlinear structure behaviors. Therefore, to investigate offshore structures in hostile sea states is necessary.

For the high cost and space limit for experiments, the numerical methods have its advantages to forecast the severe sea states and the wave-structure interactions. However, uncertainty still remains when considering the model fidelity. Thus the numerical simulation based on a benchmark test is required to ensure the accuracy of numerical methods and provide more details for future development of numerical modeling. Many researchers have discussed the nonlinear interaction between the steep waves and offshore structures (Kashiwagi, M., 2000). Yan, S. et al (2015) applied uni-directional focusing waves and a cylinder based on QALE-FEM (Quasi Arbitrary Lagrangian Eulerian Finite Element Method) with FNPT (fully nonlinear potential theory) and OpenFOAM coupled with potential theory. They compared those two methods when simulating the focusing waves and the cylinder. For the Floating Production Storage and Off-loading (FPSO) vessels are commonly used as oil storage and operate system, many studies have been done to discover the wave-structure interaction. Inoue, Y.et al (1993) used FPSO to investigate the effect of short crested waves on low frequency motions of moored tanker. Wu, G.X. and Hu, Z.Z (2004) applied the fully nonlinear potential flow formulation to study interaction between the FPSO and regular waves. As for the development of computer science, the CFD method has its ability to simulate some specific phenomenon. For example, the coupling effects between FPSO and sloshing tanks (Zhuang, Y. and Wan, D.C., 2016) and the extreme wave loading on offshore structures (Westphalen, J. et al., 2014). As the six DOF solving needs lots of cost, as well as to figure out the scattered wave and pressure on structure in detail, Mai, T. et al (2016), Hu, Z.Z. et al (2016) and Ma, Q.W. et al (2015) discussed the interaction between a fixed-body and focused waves.

In the present work, a CFD-based method is applied to simulate a fixed FPSO-shaped body in focused waves. The simulation conditions follow the settings of experiments conducted in the Ocean Basin at Plymouth University's COAST Laboratory. The fixed model is subjected to irregular wave conditions with wave height of 0.077m, a range of incident wave angles (= 0,10 &20°).

All the numerical simulations are carried out by the in-house CFD code naoe-FOAM-SJTU. Our in-house solver has developed wave maker module which can generate irregular waves like the focused wave. Firstly, the values of wave height in different position of the empty wave tank are obtained through computations. Secondly, the structure is put into the numerical tank, and the scattered waves around hull are analyzed. The pressure on the hull is also provided. The run-up on the object is studied under different wave directions. The results of the wave and the corresponding pressure on the hull are in CCP-WSI Blind Test Workshop to ensure the accuracy of the method.

METHODOLOGY

Governing Equation

The incompressible Navier-Stocks equations are adopted in this paper to investigate the viscous flow. Using dynamic deformation mesh, the governing equations are:

$$\nabla \cdot \mathbf{U} = 0 \tag{1}$$

$$\rho(\frac{\partial \mathbf{U}}{\partial t} + \mathbf{U} \bullet \nabla(\mathbf{U} - \mathbf{U}_g) = -\nabla p_d - \mathbf{g} \bullet \mathbf{x} \nabla p + \mu \nabla^2 \mathbf{U} + \mathbf{f}_\sigma + \mathbf{f}_s \tag{2}$$

Where $\mathbf{U}$ is velocity field, $\mathbf{U}_g$ is velocity of grid nodes; $p_d = p - \rho \mathbf{g} \cdot \mathbf{x}$ is dynamic pressure; $\mathbf{f}_\sigma$ is the surface tension term in two phases model.

The solution of momentum and continuity equations is implemented by using the pressure-implicit spit operator (PISO) algorithm (Issa, R.I. 1986). PISO algorithm applies mass conservation into pressure equation, thus when pressure equation converges, continuity error decreases. This method uses a predictor-corrector on solving pressure-velocity coupling, and utilizes a collocated grid method (Rhie, C.M. and Chow, W.L., 1983).

VOF Method

The Volume of fluid (VOF) method with bounded compression techniques is applied to control numerical diffusion and capture the two-phase interface efficiently. The VOF transport equation is described below:

$$\frac{\partial \alpha}{\partial t} + \nabla \bullet [(\mathbf{U} - \mathbf{U}g)\alpha] = 0 \tag{3}$$

Where α is volume of fraction, indicating the relative proportion of fluid in each cell and its value is always between zero and one:

$$\begin{cases} \alpha = 0 & \text{air} \\ \alpha = 1 & \text{water} \\ 0 < \alpha < 1 & \text{interface} \end{cases} \tag{4}$$

Wave Generation and Damping

The irregular focused wave is generated by imposing the boundary conditions of α and $\mathbf{U}$ at the inlet. Due to the adjustment of phase angle of component waves, the wave crest of the component waves can be added in a certain position and time spot to formulate the focused wave. The model of focused wave is

$$\eta(x, \mathrm{y}, t) = \sum_{i=1}^{N_f} \sum_{j=1}^{M_\theta} A_{ij} \cos[k_i(x - x_f)\cos\theta_j + k_i(y - y_f)\sin\theta_j - 2\pi f_i(t - t_f)] \tag{5}$$

When $x = x_f$, $y = y_f$, $t = t_f$, all the component wave crest will accumulate at $P_f(x_f, y_f)$. Therefore, we obtain the significant wave height to be:

$$\eta(x,t) = \sum_{i=1}^{N_f} \sum_{j=1}^{M_\theta} A_{ij} \tag{6}$$

There were three different type of distribution spectrum of wave amplitude, CWA (Constant Wave Amplitude), CWS (Constant Wave Steepness) and wave spectrum such as JONSWAP. To be consistent with the experimental setup, the wave amplitude distribution was chosen to be JONSWAP wave spectrum.

$$A_{ij} = A_f \frac{S(f_i)}{\sum_{i=1}^{N_f} S(f_i)} \tag{7}$$

NUMERICAL SIMULATION

Numerical Setup

The physical model was chosen the same as experiment done in the Ocean Basin at Plymouth University's COAST Laboratory, the structure (M3) has vertical sides and each end is semi-circular with the same radius (0.15m). The full height of the structure is 0.303m and the draft is 0.153m, shown in Fig.1. Fig.1 (a) is the setup of experiments (Mai, 2016) and (b) is physical model in numerical simulation.

Table 1 illustrates the wave parameters for both wave fields test case and fixed fpso-shaped body case. Those three cased are different on wave angle. Each wave was created using linear superposition of 244 wave fronts with frequencies evenly spaced between 0.101563Hz and 2Hz and a theoretical focus location, x0, 13.886m from the wave inlet boundary. The amplitudes of the frequency components were derived by applying a JONSWAP spectrum with the parameters in the Table 1 where Alpha is the angle of propagation relative to the centre-line of the basin and Phi is the phase of the components at the focus location.

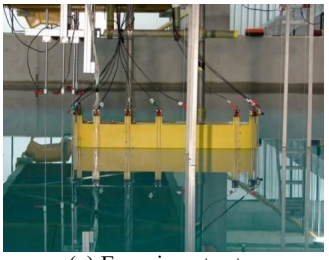

(a) Experiment setup

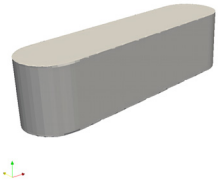

(b) Numerical model

Fig.1 Geometry of fpso-liked body.

Table 1 Wave parameters for each of the test cases

CCP-WSI ID	A	Tp	h	Hs	kA	Alpha	Phi
	(m)	(s)	(m)	(m)		(rad)	(rads)
21BT1	0.08930	1.456	2.93	0.103	0.17	0	π
22BT1	0.08930	1.456	2.93	0.103	0.17	0.174533	π

23B T1	0.08930	1.456	2.93	0.103	0.17	0.34906 6	π

The selected computational domain is described as 0m<x<23m, --2.5m<y<2.5m, -1.5m<z<1m. The meshes are generated by *snappyHexMesh*, an auto mesh generation utility provided by OpenFOAM. The mesh generations are shown in Fig. 2. The total cell number of case without model is around 2.89M, and the total cell number of case with model is around 5.8M.

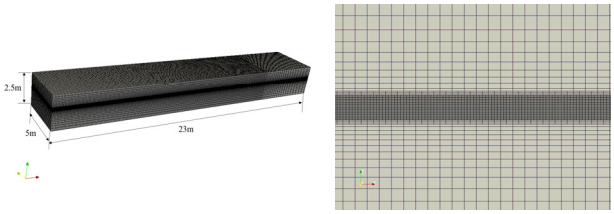

(a) Mesh of computational domain (b) Mesh of free surface

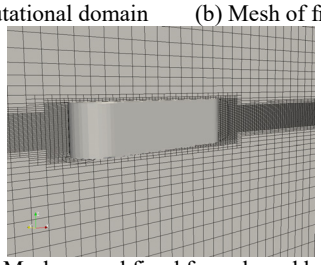

(c) Mesh around fixed fpso-shaped body

Fig. 2 Demonstrations of mesh

Fig. 3 indicates the wave gauges setup and pressure probes of current study. Those setup pictures were come from https://www.ccp-wsi.ac.uk/blind_test_series_1_focused_wave. Two different arrays of wave gauges were used for the empty tank cases (Fig. 3 (a)) and cases with the structure present (Fig. 3 (b)). An array of 9 pressure transducers were positioned on the bow of the FPSO on the centerline (P1, P2 & P3) and at 45° to the port (P7, P8 & P9) and starboard (P4, P5 & P6) sides; at the still water level and at depths of ±0.05m (Fig.3 (c)). To compare with the experimental results, wave gauge 7, 11 (on the focused position), 12 (on the focused position), 15, 16 and 17 will be analyzed. In order to analyze the wave-structure interaction in detail and to participate in the blind test, only wave gauge 15,16,17,24 and 7 will be considered. To make the wave gauge displacement more clarify, the position of identical number wave gauge in case with and without model is different. Meanwhile, time series of pressure in 1, 2, 3, 4, 6 and 8 will be analyzed.

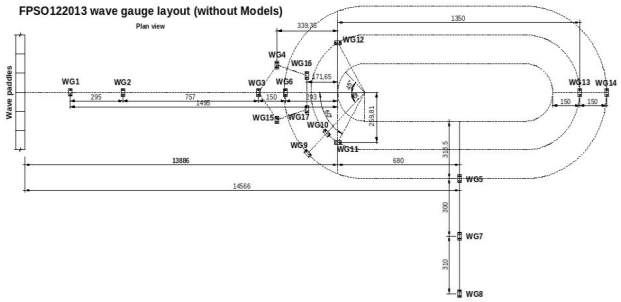

(a) Wave gauges layout in wave tank (without model)

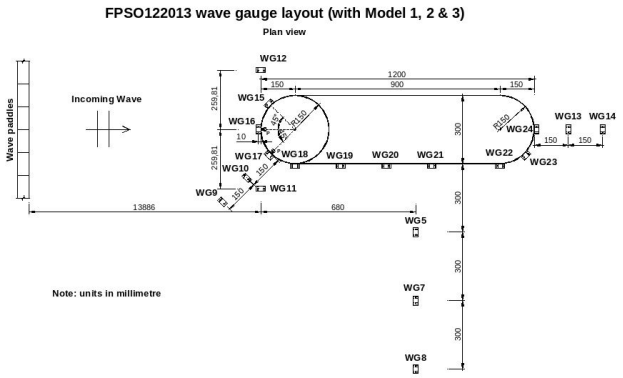

(b) Wave gauge layout (with model)

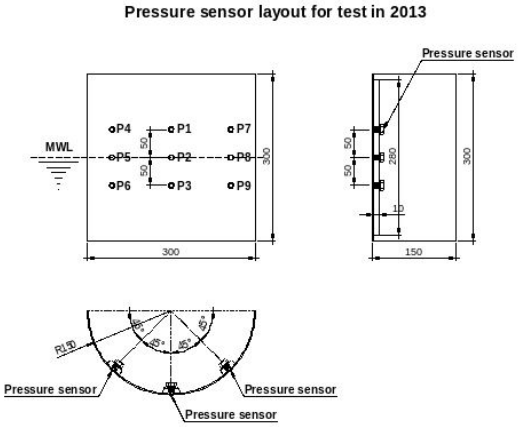

(c) Pressure sensor layout

Fig. 3 Foundation of numerical simulation

Wave Elevation Without Model

The mesh convergence and time step convergence are carried out firstly. As shown in Fig.4, three mesh grid numbers are included. The total number of grids are 1.16M, 2.89M and 6.91M respectively. The time step of these three cases are the same, $\Delta t = 0.01s$. The results of 1.16M is different from that of other two cases. While the grid number is 2.89M, the value of the wave elevation is almost the same with that of 6.91M. The mesh is converged, and in order to save computational source, the final mesh grid number is chosen to be 2.89M.

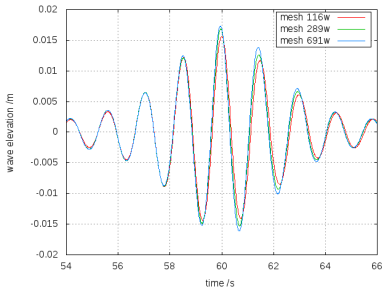

Fig. 4 Time history of mesh convergence at focused position (21BT1)

The time step convergence is illustrated in Fig.5. Three different time steps are chosen, Δt = 0.001s, 0.0005s and 0.0003s respectively. With the decrease of the time step, the value of wave amplitude increases. As the difference between case of 0.0005s and 0.0003s is not obvious (error 5%), to save computational source, the time step is chosen to be

0.0005s.

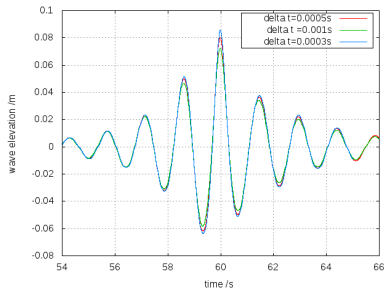

Fig. 5 Time history of time step convergence at focused position(21BT1)

The wave elevation in empty wave tank is analyzed, that is, without model inside. The wave elevation at focused position is displayed in Fig.6. The results are shown in Fig. 7, Fig. 8 and Fig. 9, illustrating wave elevation in wave angle 0 degree, 10 degree and 20 degree respectively. The results are compared with the experimental results to verify the numerical methods. It can be observed that there exists some discrepancy between present results and experimental results. The wave maker of our in-house software used velocity inlet to generate the wave, which may cause the numerical dissipation.

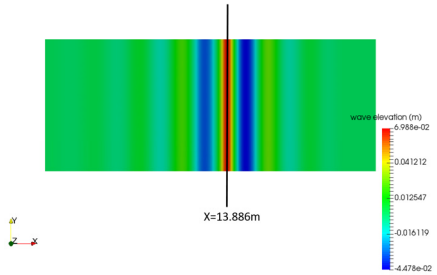

Fig. 6 Wave elevation at focused position(21BT1)

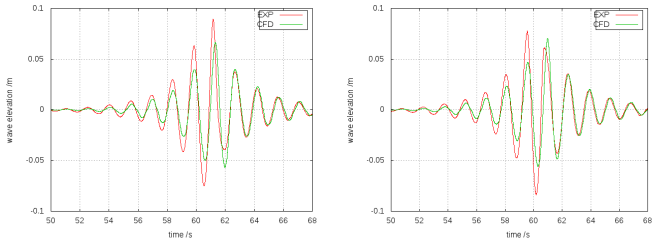

(a) Wave gauge 7 (b) Wave gauge 11

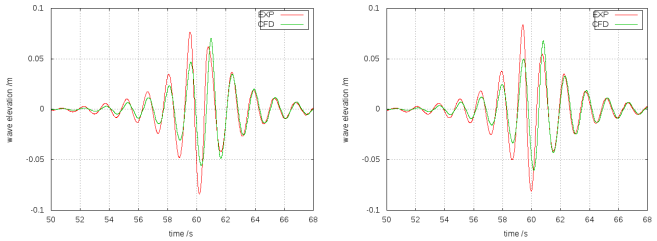

(c) Wave gauge 12 (d) Wave gauge 15

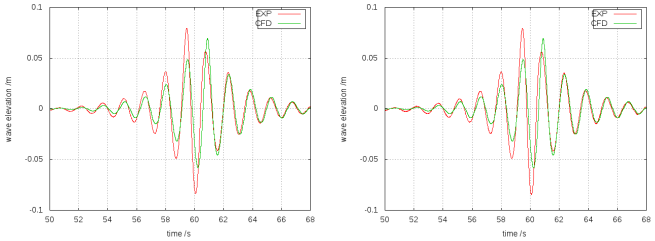

(e) Wave gauge 16 (f) Wave gauge 17

Fig. 7 Wave elevation at different wave gauges in wave angle 0 (21BT1)

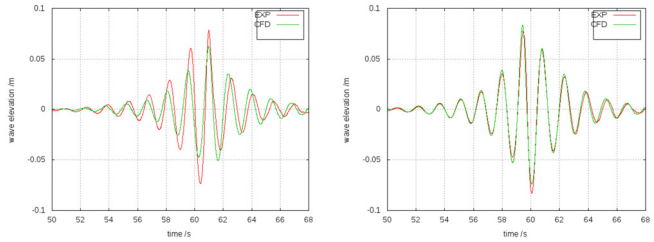

(a) Wave gauge 7 (b) Wave gauge 11

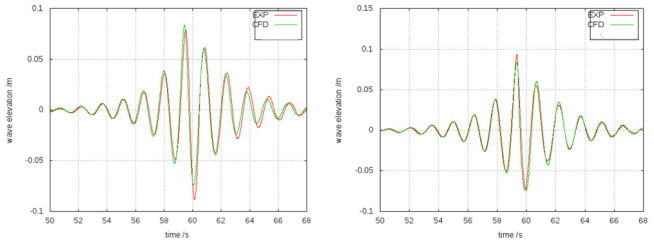

(c) Wave gauge 12 (d) Wave gauge 15

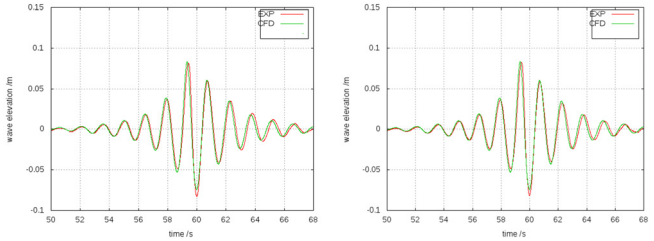

(e) Wave gauge 16 (f) Wave gauge 17

Fig. 8 Wave elevation at different wave gauges in wave angle 10 (22BT1)

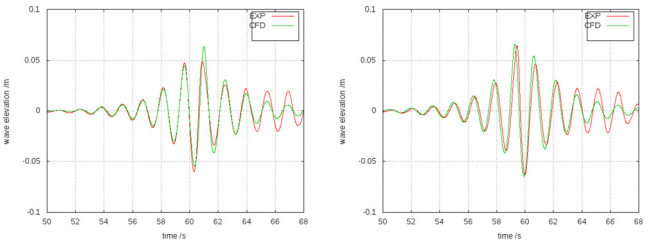

(a) Wave gauge 7 (b) Wave gauge 11

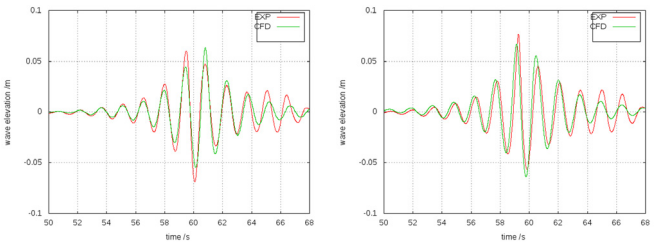

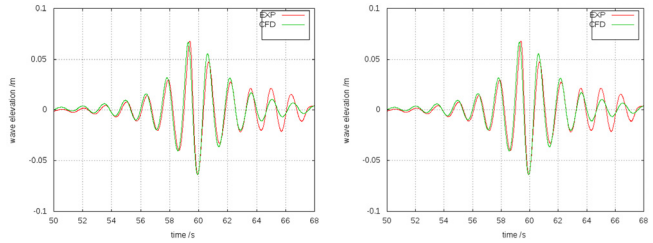

(c) Wave gauge 12 (d) Wave gauge 15

(e) Wave gauge 16 (f) Wave gauge 17

Fig. 9 Wave elevation at different wave gauges in wave angle 20 (23BT1)

The influence of wave angles on empty tank is considered, shown in Fig.10. Wave gauge 7 is placed beside the center of the wave tank, the difference is obvious. The wave elevation value and wave phase in wave angle 0 is larger than that of wave angle 10 and 20. Especially when $\alpha = 20$, the value reduces sharply at the focused time. However, in other wave gauge position, the wave phase difference in the focused position is not obvious. For wave gauge 7 is far away from centerline, the other wave gauges are set around the centerline. Therefore, it can be seen that in focused time of empty tank, the wave angle would influence the wave amplitude value, but effects wave phase little.

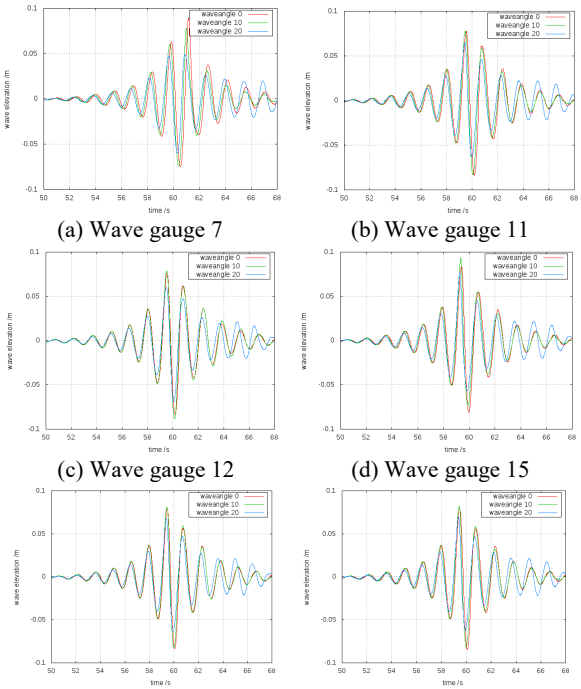

(a) Wave gauge 7 (b) Wave gauge 11

(c) Wave gauge 12 (d) Wave gauge 15

(e) Wave gauge 16 (f) Wave gauge 17

Fig. 10 Wave elevation at different wave gauges in different wave angles

Scattered Wave and Pressure around Model

The comparison of wave gauges in different wave angles are shown in Fig. 11. Wave gauge 15, 16 and 17 are placed around the model bow, wave gauge 24 is in the position of model stern and wave gauge 7 is beside the model. Although the wave gauge numbers are different with those without models, the trend of the influence of wave angles are the same. The wave elevation value and wave phase in wave angle 0 is larger than that of wave angle 10 and 20. The existence of fpso-liked body make the wave phase in oblique waves changes obviously.

It can be seen that the influence of wave angle on wave amplitude value is not proportional both in case with and without models. In Fig. 10, when there is no model inside the wave tank, the wave amplitude value when wave angle equals to 10 degree is almost the same with that of 0 degree. However, the wave amplitude of wave angle equals to 20 degree shows much difference. It is smaller than that of 10 degree and 0 degree around the focused time but become larger after the focused time. That's due to the change of distance between inlet position and focused position under different wave angles.

When it comes to the case with model in it, the wave gauge changes. Due to the existence of the model, the scattered wave amplitude is almost the same in the oblique waves, and the wave phase difference is more obvious.

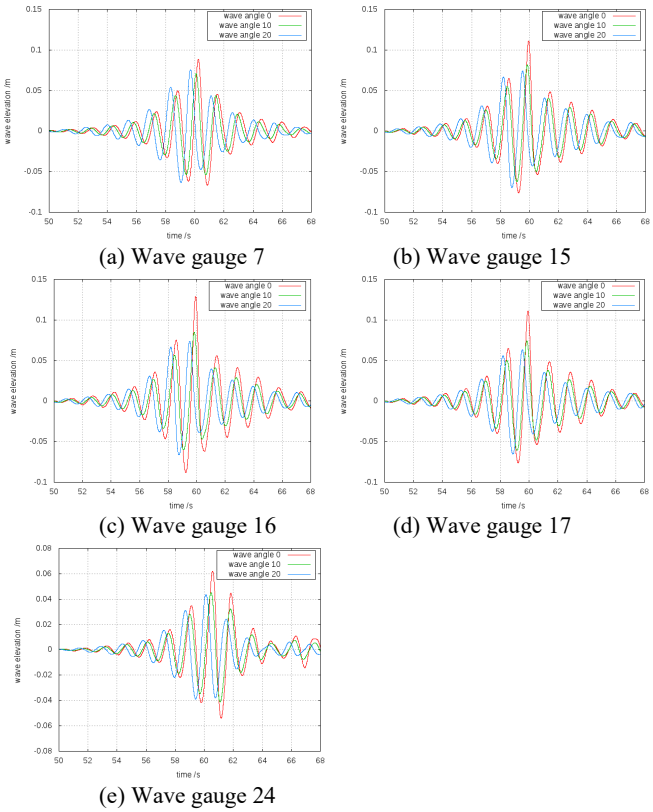

(a) Wave gauge 7 (b) Wave gauge 15

(c) Wave gauge 16 (d) Wave gauge 17

(e) Wave gauge 24

Fig.11 Time history of scattered wave elevation in different wave angles

Fig.12 illustrates the pressure on the model. Pressure probe 1 and 4 is set above the free surface. Pressure probe 2 and 8 is set on the free surface. Pressure probe 3 and 6 is set below the free surface. Pressure probe 1, 2 and 3 are set on the centerline of the model.

The value of pressure probes are nearly proportional to the wave gauge 16 and 17. For the pressure probes are put in the same place with the wave gauge 16 and 17, and as there is not impulsive pressure, the pressure are all come from the wave run-up. That is, the value of the pressure detected on the body is due to the pressure from the wave elevation. Therefore, the phase and value of the pressure is almost proportional to the scattered wave elevation.

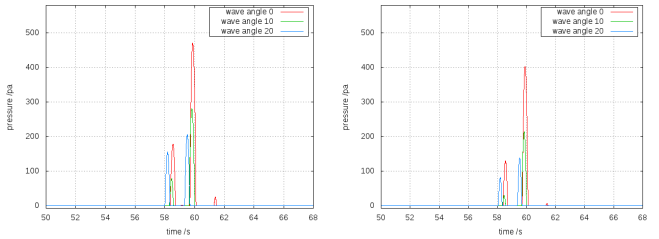

(a) Pressure p1 (b) Pressure p4

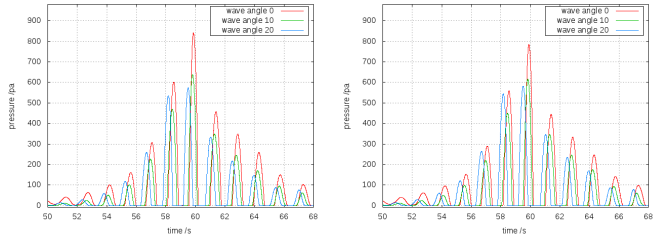

(d) Pressure p2 (e) Pressure p8

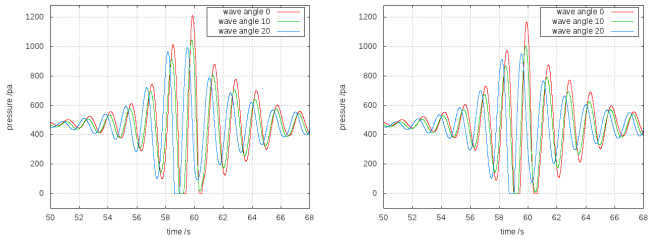

(e) Pressure p3 (f) Pressure p6

Fig.12 Time history of pressure on model in different wave angles

Pressure probe 4 is on the right side of the model bow, thus when the wave crest passing through, the bow of the model would absorb the most wave energy so the value in pressure probe 4 is smaller than that of pressure probe 1. It can be observed that in the position of pressure probe 1, the 0 degree case has a third peak after the focused time. The generation of third peak is due to the second wave crest after the focusing wave crest. The run-up of oblique wave crest is not on the position of pressure probe 1, therefore only 0 degree case can observe the third pressure peak.

Pressure probe 8 is on the left side of the model bow. Due to the reason clarified above, the value of probe 8 is smaller than that of probe 2 when wave angle equals to 0. However, on the oblique wave condition, the value of probe 8 is nearly the same with that of probe 2, and when wave angle equals to 20, the value is closer. After wave crest impact on the model, the wave energy reduces when it split into two sides. For the wave angle equals to 20 degree, the distance from probe 8 and probe 2 to the impact point is close, thus there is not much difference between these two pressure values.

The value in probe 3 and probe 6 does not show much difference. Probe 6 is on the right side of the model bow. Thus the trend of the pressure value is the same with that in probe 4. The pressure value trend and scattered wave amplitude trend can be verified in Fig. 13. As shown in Fig.13, the snapshots of wave run-up in three different incident wave angles. The wave split is symmetrical in wave angle 0 degree, while is asymmetrical in oblique wave conditions.

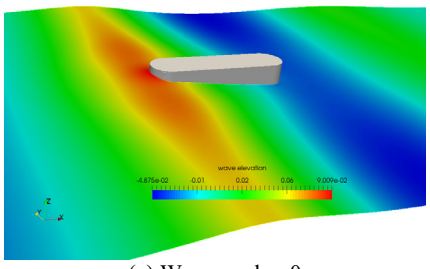

(a) Wave angle =0

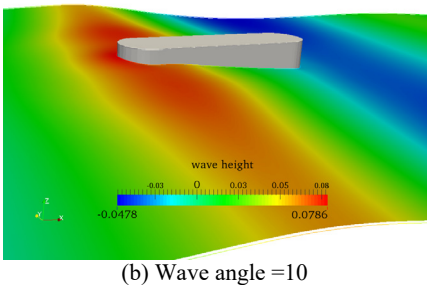

(b) Wave angle =10

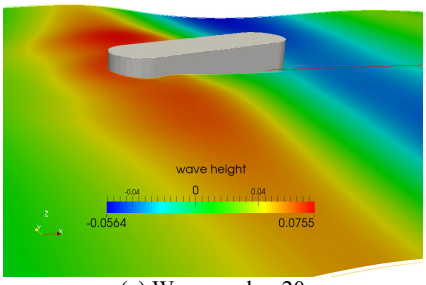

(c) Wave angle =20

Fig. 13 Snapshots of wave run-up on model

CONCLUSIONS

This paper applied CFD method using our in house solver naoe-FOAM-SJTU to generate focsed waves and solved a fixed fpso-like model under the focued wave. The physical model is chosen from a benchmark test. Firstly, the wave elevation of empty wave tank is simulated. Three different incident wave angles are considered. The mesh convergence and time step convergence are carried out. The results are compared with the experimental results. The comparison results show fair agreement although with some discrepancies. Then the model is placed inside the tank, the scattered wave elevation and pressure on model are calculated.

The influence of different incident wave angle on scattered wave elevation and pressure on model are discussed. The incident wave angle would affect the maximum wave crest and wave loading. With model inside, the split point of wave would change with the incident wave angle, thus the wave load and wave phase in the same wave probe position and pressure position is different.

The discrepancy between present work and experimental results are

under consideration. Since the mesh and time step convergence have carried out, the choice of different numerical discretization scheme is considered to achieve better results.

ACKNOWLEDGEMENTS

This work is supported by the National Natural Science Foundation of China (51490675, 11432009, 51579145), Chang Jiang Scholars Program (T2014099), Shanghai Excellent Academic Leaders Program (17XD1402300), Program for Professor of Special Appointment (Eastern Scholar) at Shanghai Institutions of Higher Learning (2013022), Innovative Special Project of Numerical Tank of Ministry of Industry and Information Technology of China (2016-23/09) and Lloyd's Register Foundation for doctoral student, to which the authors are most grateful.

REFERENCES

Hu Z.Z., Mai T., Greaves D., Raby A. (2016, June). "A Numerical and Experimental Study of a Simplified FPSO in Extreme Free Surface Waves." *In The 26th International Ocean and Polar Engineering Conference. International Society of Offshore and Polar Engineers*. Rhodes, Greece, 1103-1109.

Inoue Y., Xue W., Yamagishi N., Yokozawa H.(1993) "Low frequency motions of FPSO in short and long crested waves." *The Third International Offshore and Polar Engineering Conference. International Society of Offshore and Polar Engineers,* ISOPE, Singapore, 93-262.

Issa R.I (1986). "Solution of the implicitly discretized fluid flow equations by operator-splitting," *Journal of computational physics,* 62(1), 40-65.

Kashiwagi M. (2000). "Nonlinear simulations of wave-induced motions of a floating body by means of the mixed Eulerian– Lagrangian method." *Proceedings of the Institution of Mechanical Engineers. Part C, Journal of Mechanical Engineering Science*, 214,841–855

Ma Q.W., Yan S., Greaves D., Mai T., Raby A. (2015, July). "Numerical and experimental studies of Interaction between FPSO and focusing waves." *In The Twenty-fifth International Ocean and Polar Engineering Conference. International Society of Offshore and Polar Engineers.* Kona, Big Island, Hawaii, USA, 655-662.

Mai T., Greaves D., Raby A., Taylor P.H. (2016). "Physical modelling of wave scattering around fixed FPSO-shaped bodies." *Applied Ocean Research*, 61, 115-129.

Rhie C.M., Chow W.L. (1983). "Numerical study of the turbulent flow past an airfoil with trailing edge separation." *J AIAA journal*, 21(11), 1525-1532.

Westphalen J., Greaves D.M., Raby A., Hu Z.Z., Causon D.M., Mingham C.G., Omidvar P., Stansby P.K., Rogers B.D (2014)."Investigation of wave-structure interaction using state of the artCFD techniques," Open Journal of Fluid Dynamics, 4(1). 18-43.

Wu G.X., Hu Z.Z (2004). "Simulation of nonlinear interactions between waves and floating bodies through a finite element based numerical tank," *Proceedings of the Royal Society* A, 460, 2797-2817.

Yan S, Ma Q.W, Sriram V, Qian L., Ferrer P.J.M., Schlurmann T. (2015). "Numerical and Experimental Studies of Moving Cylinder in Uni-directional Focusing Waves", *The Twenty-fifth International Ocean and Polar Engineering Conference*, ISOPE. Kona, Hawaii, USA. 51-59.

Zhuang Y., Wan D.C.(2016) "Numerical study on coupling effects of FPSO ship motion and LNG tank sloshing in low-filling condition". *Applied Mathematics and Mechanics*, 37(12): 1378-1393.